Search for heavy neutrinos in a 3-lepton final-state

Applications using supervised machine learning

by

William Hirst

THESIS

for the degree of

MASTER OF SCIENCE

Faculty of Mathematics and Natural Sciences
University of Oslo

Autumn 2022

Search for heavy neutrinos in a 3-lepton final-state

Applications using supervised machine learning

William Hirst

Search for heavy neutrinos in a 3-lepton final-state

http://www.duo.uio.no/

Printed: Reprosentralen, University of Oslo

Abstract

This will be the abstract.

Acknowledgments

First of all I would like to thank my supervisor, Are Raklev, for giving me the trust and encouragement to explore what I found most fascinating on the subject of this thesis. Your enthusiasm for physics and dedication to detail has been of enormous value. I am grateful that you always found time to answer my questions and put me back on track. I also wish to thank Anders Kvellestad, Jeriek Vda and Eli Rye for all the help and encouragement.

Thanks to the whole theory group for making these last years so enjoyable, and a special thanks to Cecilie Glittum, a good friend and vital physics-partner the last five years. I also would like to thank Kristian Wold, Lars Dean and Jonathan Waters for all the fruitful knowledge exchanges and especially for the warm friendships. Many thanks to my family, for always supporting and believing in me.

Finally, huge thanks to my girlfriend Elin. Words cannot describe how grateful I am for all her love, support and patience. This thesis would not have been possible without her.

Contents

Introduction

The standard model (SM) is perhaps one of the most successful scientific theories ever created. It accurately explains the interactions of leptons and quarks as well as the force carrying particles which mediate said interactions. In 2012 the SM achieved one of its crowning achievements when we discovered the Higgs boson. Much of the accolade was rightfully given to the theoretical work on the SM, but another aspect of the discovery was equally important. Data analysis was and is a crucial part of any new discovery in physics. One of the most important and exiting tools is machine learning.

Outline of the Thesis

Chapter 1

The Standard model of elementary particles

The standard model (SM) is perhaps one of the most successful scientific theories ever created. It accurately explains the interactions of leptons and quarks as well as the force carrying particles which mediate said interactions. In 2012 the SM achieved one of its crowning achievements when we discovered the Higgs boson.

1.1 Phenomenology - What is it?

1.2 The background channels

The dominant SM backgrounds can be divided into two categories: (i) from leptonic τ decays and (ii) from fake leptons. In the first category, the dominant process is the pair production of WZ with W decaying leptonically and $Z \to \tau\tau$. The trilepton final states with no-OSSF pairs can arise from the subsequent leptonic decay of τ 's. We estimate this background process via Monte Carlo simulations.
The dominant processes of the second category are $\gamma^*/Z+$ jets and $t\bar{t}$, where two leptons come from $\gamma^*/Z \to \tau\tau$ or the prompt decay of t and $\bar{t}$, and a third lepton is faked from jets containing heavy-flavor mesons.

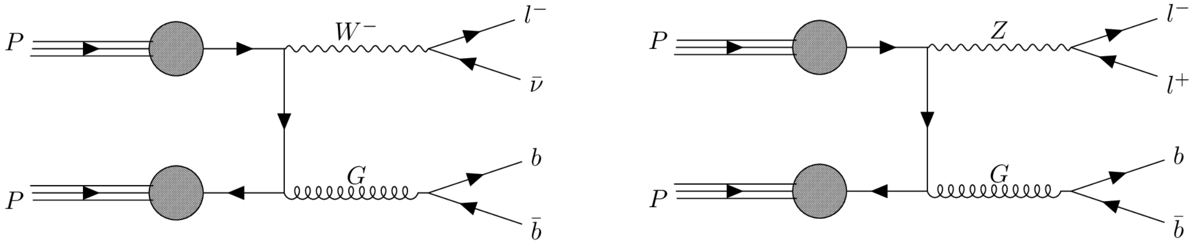

(a) (b)

Figure 1.1: The Feynman diagram of both the W+jets 1.1a and the W+jets 1.1b.

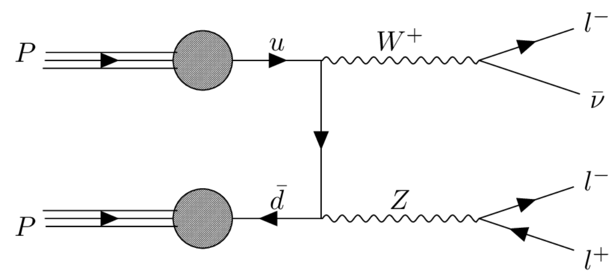

Figure 1.2: The Feynman diagram of the diboson WZ-channel.

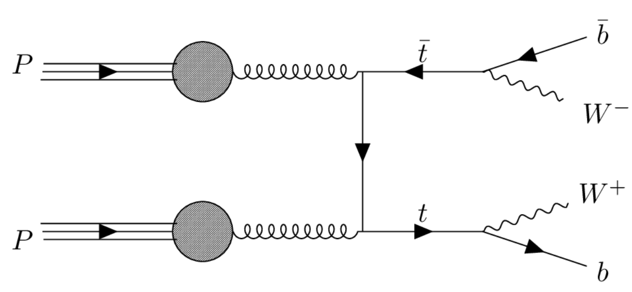

Figure 1.3: The Feynman diagram of the $t\bar{t}$-channel.

Chapter 2

Beyond the standard model - Heavy neutrinos

2.1 Why look beyond?

2.2 Neutrinos

2.3 Dirac and Majorana

2.3.1 How to distinguish the two?

Chapter 3

Statistical and multi-variabel analysis

The standard model (SM) is perhaps one of the most successful scientific theories ever created. It accurately explains the interactions of leptons and quarks as well as the force carrying particles which mediate said interactions. In 2012 the SM achieved one of its crowning achievements when we discovered the Higgs boson. Much of the accolade was rightfully given to the theoretical work on the SM, but another aspect of the discovery was equally important. Data analysis was and is a crucial part of any new discovery in physics. One of the most important and exiting tools is machine learning.

3.1 Discovery and significance

3.2 Exclusion

3.2.1 Likelihood

3.3 High- and Low-level features

Chapter 4

Introduction to supervised and unsuperised machine learning

This will give a brief intoruction to the concept of machine learning as well as the difference between supervised and unsuperised.

4.1 Neural Networks in physics

4.1.1 Deep vs Shallow networks

4.2 Gradient Boosting and decision trees

In this rapport I will use the XGBoost-classifier which uses gradient-boosted trees. Gradient-boosting is a machine learning algorithm which uses a collective of ”weak” classifiers in order to create one strong classifier. In the case of gradient-boosted trees the weak classifiers are a collective of shallow trees, which combine to form a classifiers that allows for deeper learning. As is the case for most gradient-boosting techniques, the collecting of weak classifiers is an iterative process.
We define an imperfect model $\mathcal{F}_m$, which is a collective of m number of weak classifiers, estimators. A prediction for the model on a given data-points, x_i is defined as $\mathcal{F}_m(x_i)$, and the observed value for the aforementioned data is defined as y_i. The goal of the iterative process is to minimize some cost-function $\mathcal{C}$ by introducing a new estimator h_m to compensate for any error, $\mathcal{C}(\mathcal{F}_m(x_i), y_i)$. In other words we define the new estimator as:

$$\tilde{\mathcal{C}}(\mathcal{F}_m(x_i), y_i) = h_m(x_i), \tag{4.1}$$

where we define $\tilde{\mathcal{C}}$ as some relation defined between the observed and predicted values such that when added to the initial prediction we minimize $\mathcal{C}$.
Using our new estimator h_m, we can now define a new model as

$$\mathcal{F}_{m+1}(x_i) = \mathcal{F}_m + h_m(x_i). \tag{4.2}$$

The XGBoost [**?**] framework used in this analysis enables a gradient-boosted algorithm, and was initially created for the Higgs ML challenge. Since the challenge, XGBoost has become a favorite for many in the ML community and has later won many other ML challenges. XGBoost often outperforms ordinary decision trees, but what is gains in results it looses in interpretability. A single tree can easily be analysed and dissected, but when the number of trees increases this becomes harder.

Chapter 5

Implementation

5.1 Features

The choice of which features to study and which to neglect are crucial in a search for new physics. This is particilarly true in the case of applying machine learning. The general motivation for including a given feature can be based on several factors. The first being its ability to provide a trend which we as researches can exploit when creating our regions. By this I mean that it is a variable were there is divirsity in distribution between the different channels. The second motivation is grounded in physics. Often we as physicsts tend to lean towards variables we know have some effect one the physics we are studying. For example the variable E_T^{miss}, can be directly used to either include or discard events were we do or do not expect final states with sufficent missing energy. The final motivation is grounded in the MC-simmulations ability to represent the variable. If there seems to be a clear deviation between the real and MC-data which does not stem from any new physics, we tend to discard them from the analysis.

5.1.1 Cuts and triggers

5.1.2 Lepton variables selection

Now we will have a look at what variables from the leptons that were included in the analysis. All low level information on the momentum of the leptons were added into the dataset: i.e the transverse momentum P_t, the pseudo rapidity η and the azimuthal angle ϕ. All momentum features were represented individually for each lepton. For example P_t was added as three columns, $P_t(l_1)$, $P_t(l_2)$ and $P_t(l_3)$, where the ordering of the leptons were based on the momentum from highest (l_1) to lowest (l_3). Similarly I added information regarding the charge ($\pm$) and flavor (electron, muon) of each lepton. Based on the momentum variables the transverse mass m_t of each lepoton was calculated and included along with the energy E_t^{miss} and azimuthal angle ϕ^{miss} of the missing transverse momentum.
The variables described in the section above are often considered as low-level features. These are very useful in many (if not all) searches and contribute little to no bias to your analysis. But, in the case of final-state spesific searches such as mine, one can allow one self of adding physics motivated higher-level physics. The higher level features calculated in this thesis were inspired by [1] (ATLAS 2022).
Firstly I added different mass variables, namely m_{lll} and $m_{ll}(OSSF)$. The first being the trilepton invariant mass and the latter being the dilepton invariant mass of the pair with OSSF. In the case of more than one possible OSSF-pair, the pair with the highest invariant mass was chosen. Secondly I added variables composed of the sum of different set of momentum. These variables are the sum of all three leptons $H_t(lll)$, of the pair with opposite sign $H_t(SS)$ and the sum of the momentum for all three leptons added with the missing transverse energy $H_t(lll) + E_t^{miss}$. Finally I added the significance of the E_t^{miss}, $S(E_t^{miss})$.

5.1.3 Jet variables selection

Now we can have a look at the jet-features. Given the final-state of interest should be independant of jets, there are not many features added with jet information. But, given the risk of missidentification and errors in reconstruction, some features were added. The first features were the number of jets, both all signal jets and number of b-jets. The latter information was divided in two columns based on the efficency of a multivarant analysis used to sepereata jet-flavors. The effeciencies used are 77% and %85. The last information added for the jets were the mass of the leading pair (based on p_t) di-jet mass.

5.1.4 Validation

As mentioned in previous sections, the comparison between MC- and real data is a crucial part of the analysis, and we must therefore insure an adequate reconstruction of the real data. This is not only true for the low-level features taken directly from the MC simulation, but also for the the higher-level features. Therefore we will in this section compare both sets of data for all features included in the anlysis.

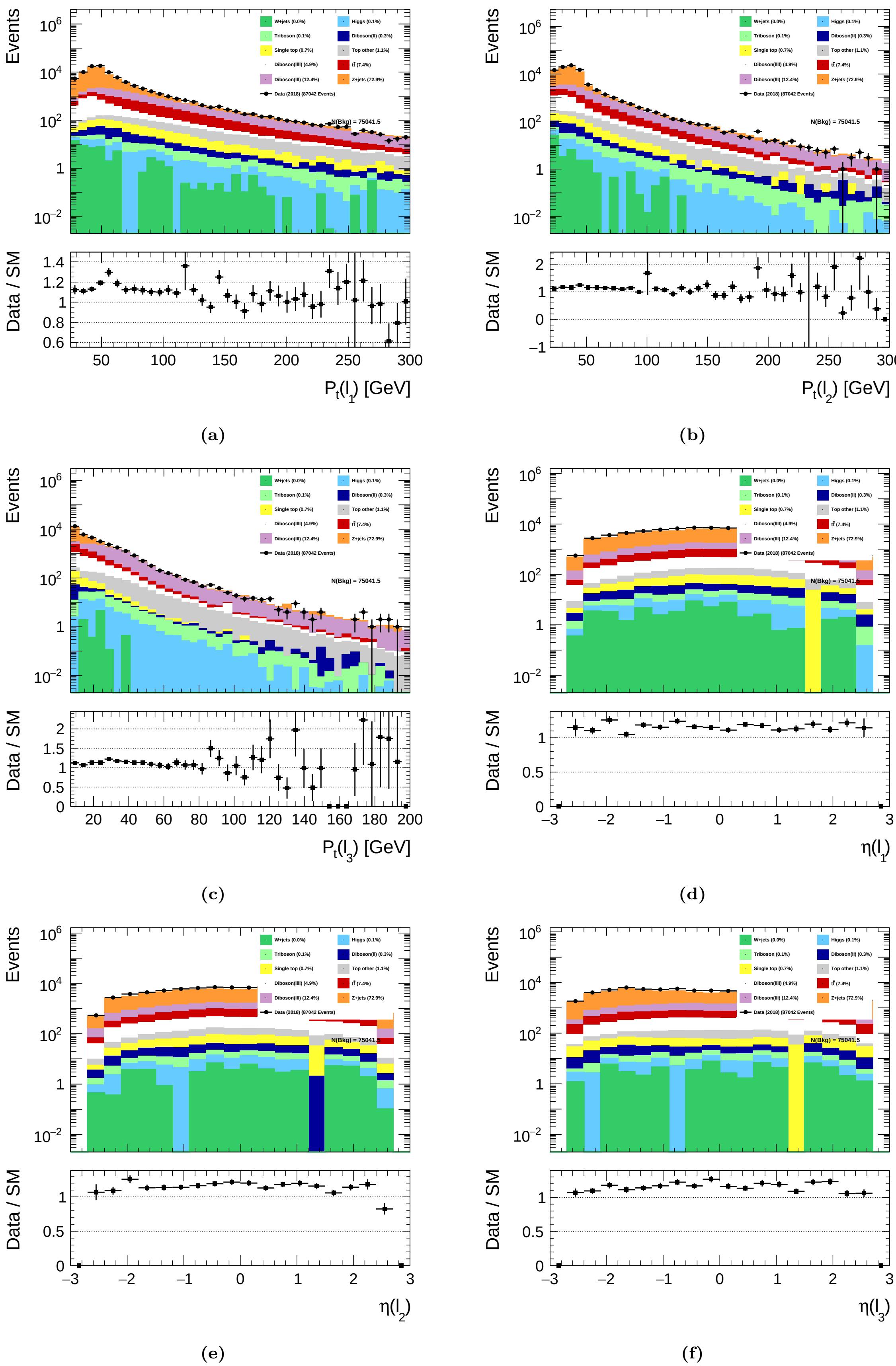

Figure 5.1: The event distribution for for each channel over P_t for the first 5.1a , second 5.1b and third 5.1c lepton. Similarly the distribution over η for the 5.1d, second 5.1e and third 5.1f lepton

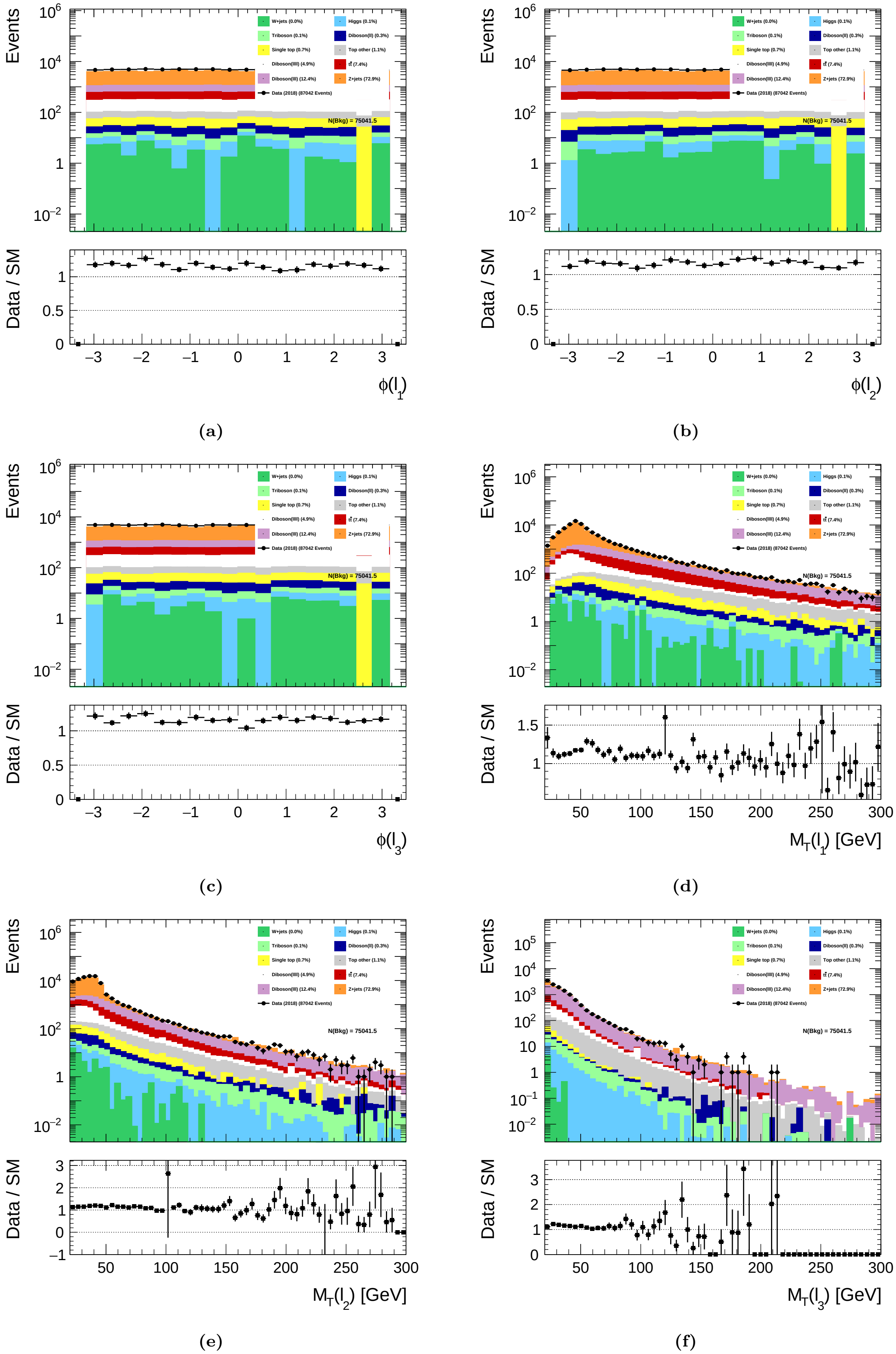

Figure 5.2: The event distribution for for each channel over ϕ for the first 5.2a , second 5.2b and third 5.2c lepton. Similarly the distribution over m_t for the first 5.2d, second 5.2e and third 5.2f lepton

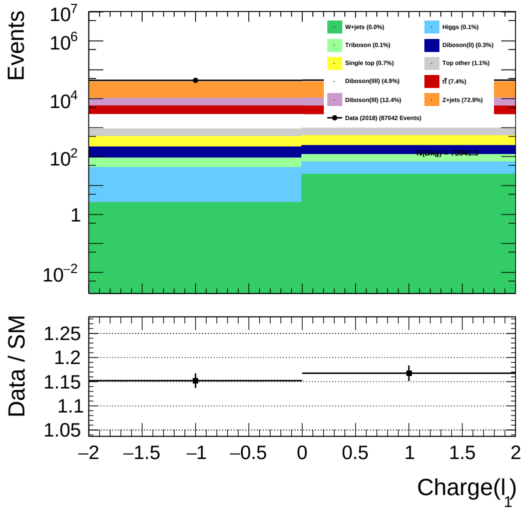

(a)

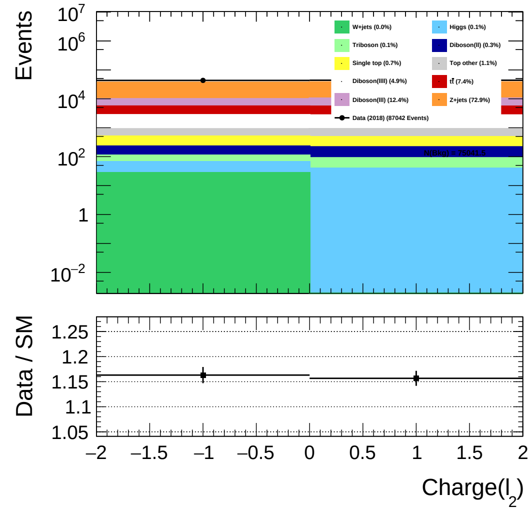

(b)

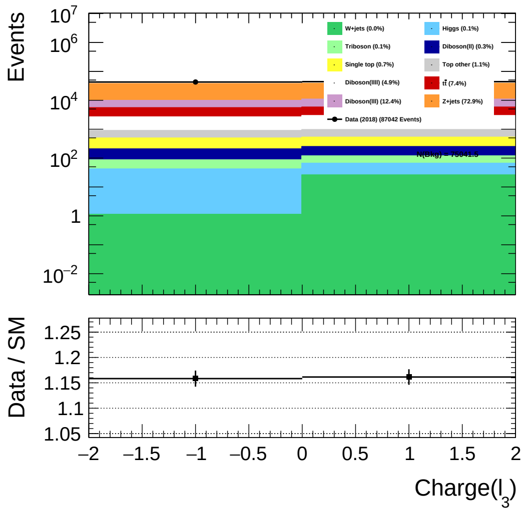

(c)

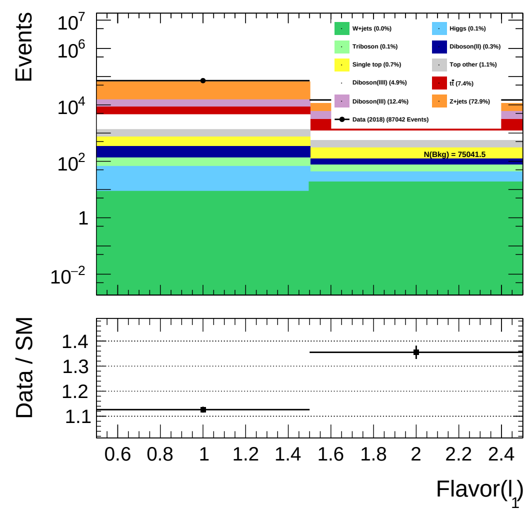

(d)

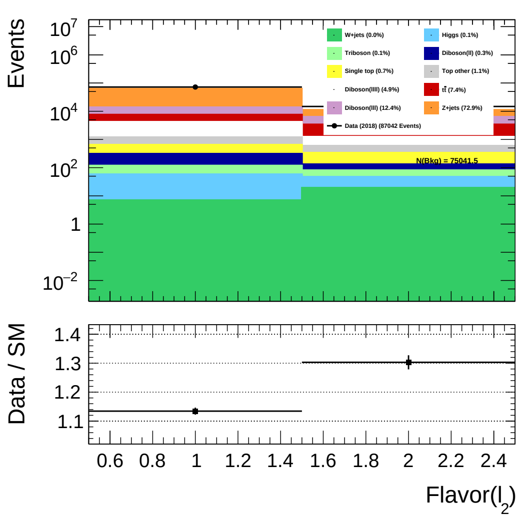

(e)

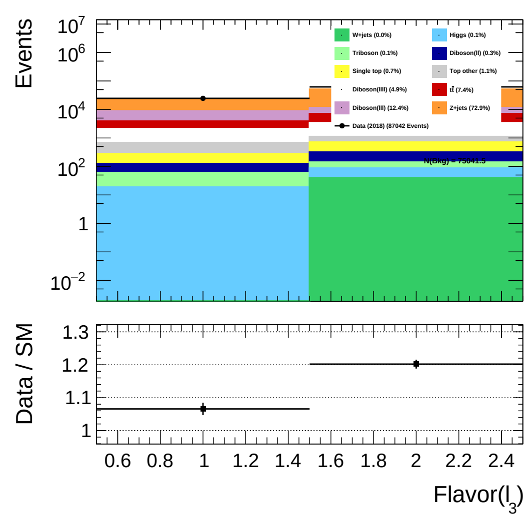

(f)

Figure 5.3: The event distribution for for each channel over the charge for the first 5.3a , second 5.3b and third 5.3c lepton. Similarly the distribution over the flavor for the first 5.3d, second 5.3e and third 5.3f lepton

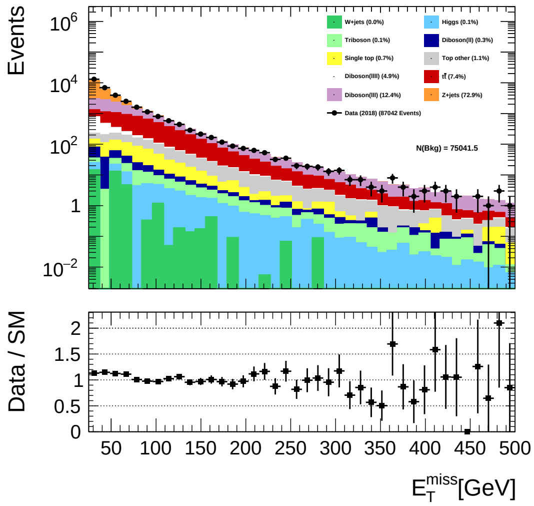

(a)

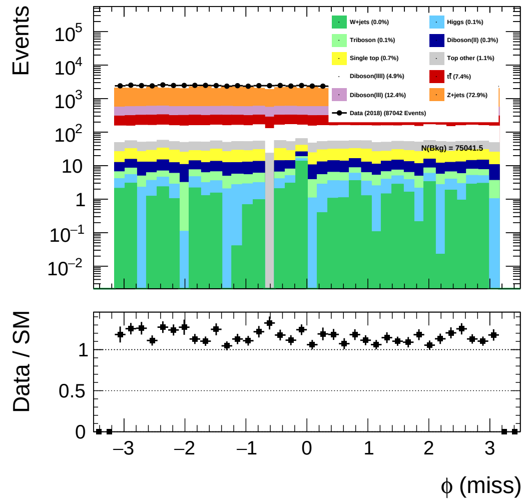

(b)

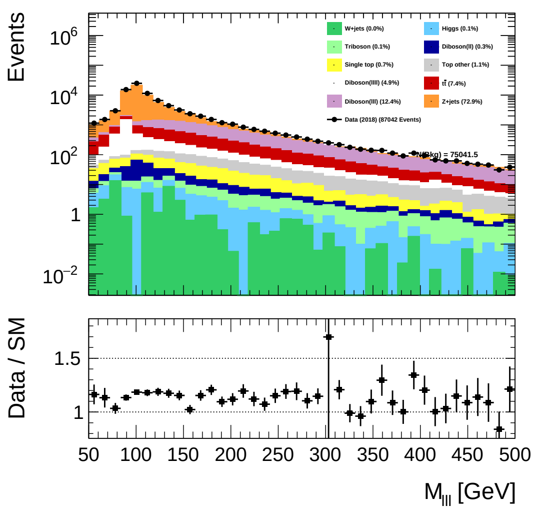

(c)

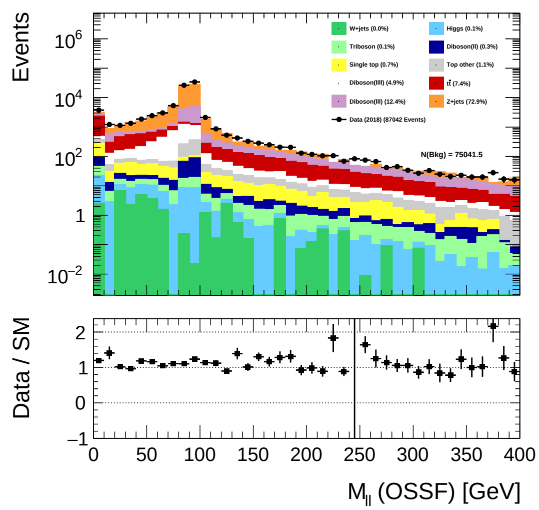

(d)

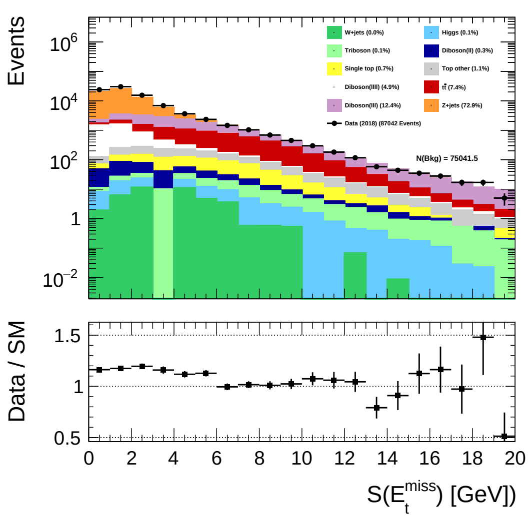

(e)

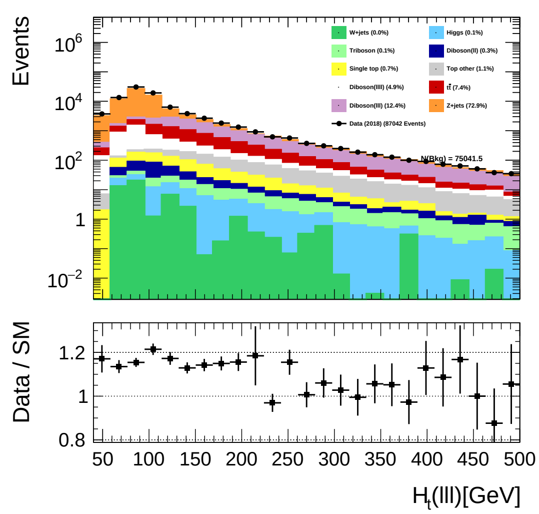

(f)

Figure 5.4: The event distribution for for each channel over the energy 5.4a and azimuthal angel 5.4b for the transverse momentum. The distribution of the invariant mass of the three leptons 5.4c and the OSSF pair 5.4d. The distribution over the significance of the missing transverse enegy 5.4e and the sum of P_t 5.4f.

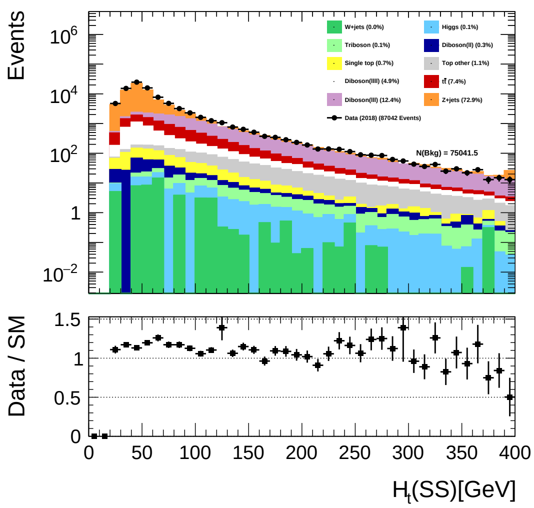

(a)

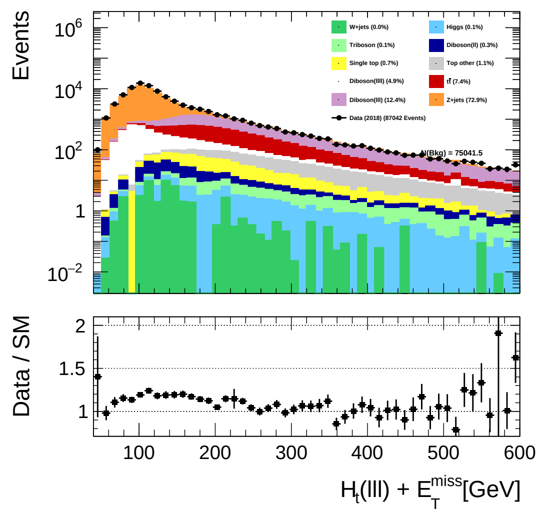

(b)

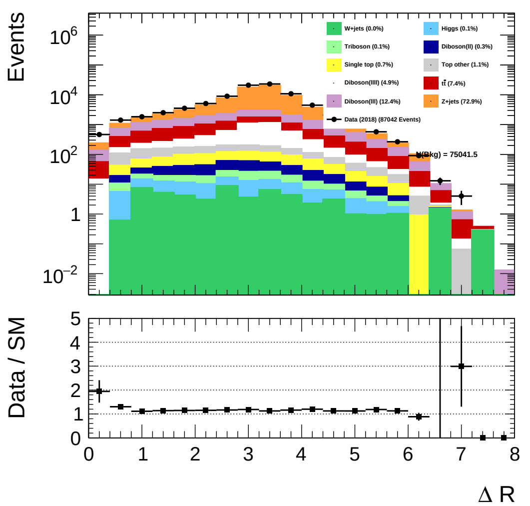

(c)

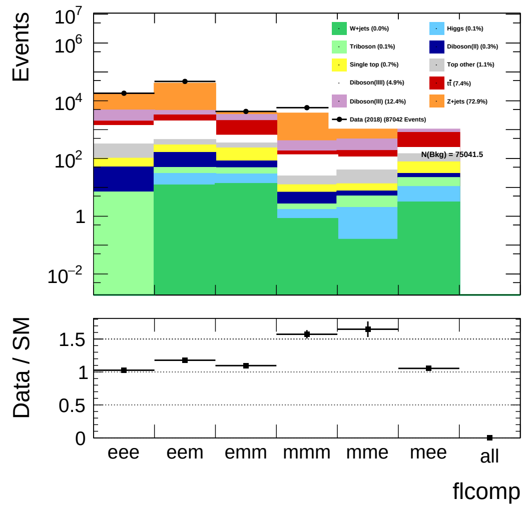

(d)

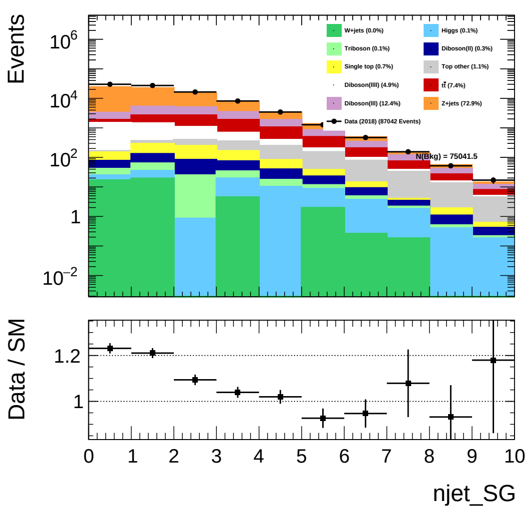

(e)

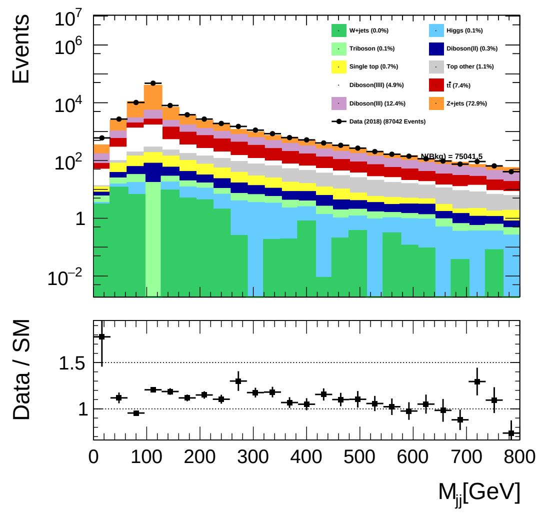

(f)

Figure 5.5: The event distribution for for each channel over the sum of P_t for the SS pair 5.5a and the sum over all three leptons added with E_t^{miss} 5.5b. The distribution over ΔR 5.5c and the flavor combination of the three leptons 5.5d. The distribution of number of jets 5.5e and the mass of the leading di-jet pair 5.5f.

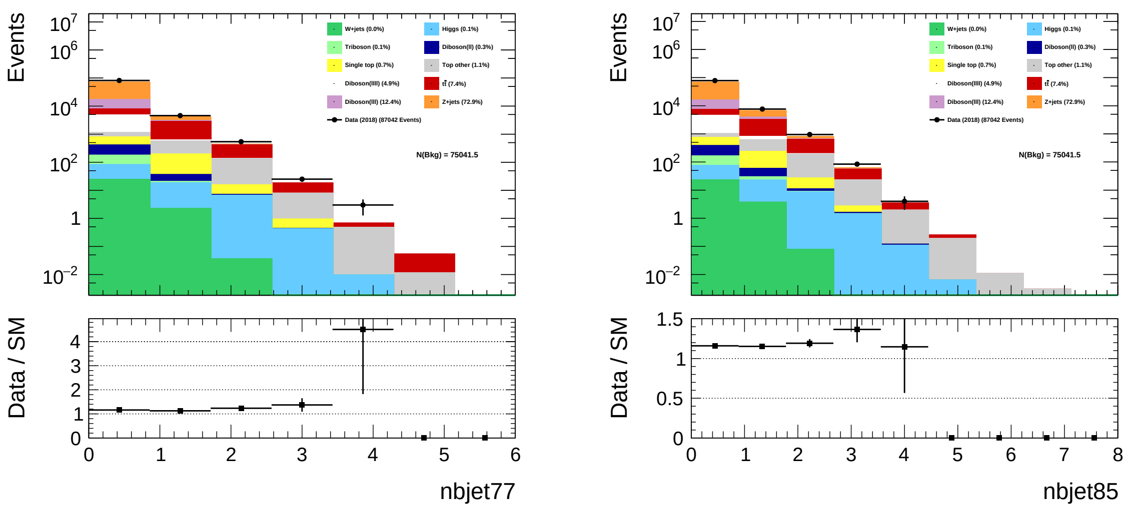

(a) **(b)**

Figure 5.6: The event distribution for for each channel over the number of b-jets with 77% 5.6a and 85% 5.6b efficency.

Appendices

Appendix A

A.1 Light-Cone Coordinates

Light-cone coordinates is specifically useful in high energy scattering processes where one want to decompose the momentum of the involving particles. For a general four vector p^μ, one defines

$$p^\mu = (p^+, p^-, p_\perp)\,, \tag{A.1}$$

where

$$p^+ = \frac{1}{\sqrt{2}}(p^0 + p^3) \tag{A.2}$$

$$p^- = \frac{1}{\sqrt{2}}(p^0 - p^3) \tag{A.3}$$

$$p_\perp = (p^1, p^2)\,. \tag{A.4}$$

Scalar products are given by

$$p \cdot k = p^+k^- + p^-k^+ - p_\perp \cdot k_\perp \tag{A.5}$$

$$p^2 = 2p^+p^- - p_\perp^2\,, \tag{A.6}$$

where the transverse contraction $p_\perp \cdot k_\perp$ is understood from the definition of the transverse vector and must not be mistaken as the same as the four momentum contraction $p \cdot k$. We will usually parametrize our momenta in terms of plus-components and from Eq. (A.6) it follows that the minus component can be written as

$$p^- = \frac{p^2 + p_\perp^2}{2p^+}\,. \tag{A.7}$$

The d-dimensional Jacobian takes the form

$$d^dp = dp^+dp^-d^{d-2}p_\perp\,. \tag{A.8}$$

From the above relations the light-cone metric takes the form

$$g_{\mathrm{LC}}^{\mu\nu} = \begin{pmatrix} 0 & 1 & 0 & 0 \\ 1 & 0 & 0 & 0 \\ 0 & 0 & -1 & 0 \\ 0 & 0 & 0 & -1 \end{pmatrix}\,, \tag{A.9}$$

where the index runs over $\mu = +, -, 1, 2$. We will elsewhere drop the subscript LC as it will always be clear from the context when we are using light-cone coordinates. One can also define light-like basis vectors

$$n_+^\mu = (1^+, 0^-, 0_\perp)\,, \qquad n_{+\,\mu} = (0^+, 1^-, 0_\perp)\,, \tag{A.10}$$

$$n_-^\mu = (0^+, 1^-, 0_\perp)\,, \qquad n_{-\,\mu} = (1^+, 0^-, 0_\perp)\,, \tag{A.11}$$

giving

$$n_+^2 = 0\,, \qquad n_-^2 = 0\,, \qquad n_+ \cdot n_- = 1\,. \tag{A.12}$$

These basis vectors project out the following components of a vector

$$p \cdot n_{+} = p^{-} \,, \qquad p \cdot n_{-} = p^{+} \,. \tag{A.13}$$

We can also construct a transversal metric

$$g_{\perp}^{\mu\nu} = g^{\mu\nu} - \left(n_{+}^{\mu} n_{-}^{\nu} + n_{+}^{\nu} n_{-}^{\mu}\right) = \begin{pmatrix} 0 & 0 & 0 & 0 \\ 0 & 0 & 0 & 0 \\ 0 & 0 & -1 & 0 \\ 0 & 0 & 0 & -1 \end{pmatrix} \,, \tag{A.14}$$

from which it follows that

$$g_{\perp}^{\mu\nu} g_{\perp\,\mu\nu} = 2 \,. \tag{A.15}$$

We can also define the gluon polarization sum in light-cone gauge, i.e $A^{+} = 0$, as

$$\sum_{\text{pol}} \varepsilon_{\alpha}(k') \varepsilon_{\beta}^{*}(k') = -g_{\alpha\beta} + \frac{k'_{\alpha}\, n_{-\,\beta}}{k' \cdot n_{-}} + \frac{k'_{\beta}\, n_{-\,\alpha}}{k' \cdot n_{-}} \,. \tag{A.16}$$

Bibliography

[1] M. Franchini, K. H. Mankinen, G. Carratta, F. Scutti, A. Gorisek, E. Lytken et al., *Search for type-III seesaw heavy leptons in dilepton final states in pp collisions at $\sqrt{s}$ = 13 TeV with the ATLAS detector*, .